

***Graphene Oxide-based Degradation of Metaldehyde: Effective Oxidation Through a Modified Fenton's Process***

*Linh Viet Nguyen<sup>a,b,c</sup>, Rosa Busquets<sup>b,d\*</sup>, Santanu Ray<sup>b</sup> and Andrew B. Cundy<sup>b,e</sup>*

L.V. Nguyen

<sup>a</sup>Department of Physical and Environmental Sciences, University of Toronto, 1265 Military Trail, Toronto, ON, M1C 1A4, Canada.

<sup>b</sup>School of Environment and Technology, University of Brighton, Brighton, East Sussex, BN2 4GJ, United Kingdom.

<sup>c</sup>Ho Chi Minh University of Natural Resources and Environment, 236B Le Van Sy, Ward 1, Tan Binh District, Ho Chi Minh City, 70000, Vietnam. Present address.

E-mail: [Vietlinh.nguyen@mail.utoronto.ca](mailto:Vietlinh.nguyen@mail.utoronto.ca)

Dr. R. Busquets\*

<sup>d</sup>Faculty of Science Engineering and Computing, Kingston University, Kingston Upon Thames, Surrey, KT1 2EE, United Kingdom. Present address.

Email: [R.Busquets@Kingston.ac.uk](mailto:R.Busquets@Kingston.ac.uk)

<sup>b</sup>School of Environment and Technology, University of Brighton, Brighton, East Sussex, BN2 4GJ, United Kingdom.

Dr. Santanu Ray

<sup>b</sup>School of Environment and Technology, University of Brighton, Brighton, East Sussex, BN2 4GJ, United Kingdom.

Email: [S.Ray4@Brighton.ac.uk](mailto:S.Ray4@Brighton.ac.uk)

Prof. Andrew B. Cundy

<sup>e</sup>School of Ocean and Earth Science, University of Southampton, Southampton, SO14 3ZH, United Kingdom. Present address.

Email: [A.Cundy@soton.ac.uk](mailto:A.Cundy@soton.ac.uk)

<sup>b</sup>School of Environment and Technology, University of Brighton, Brighton, East Sussex, BN2 4GJ, United Kingdom.

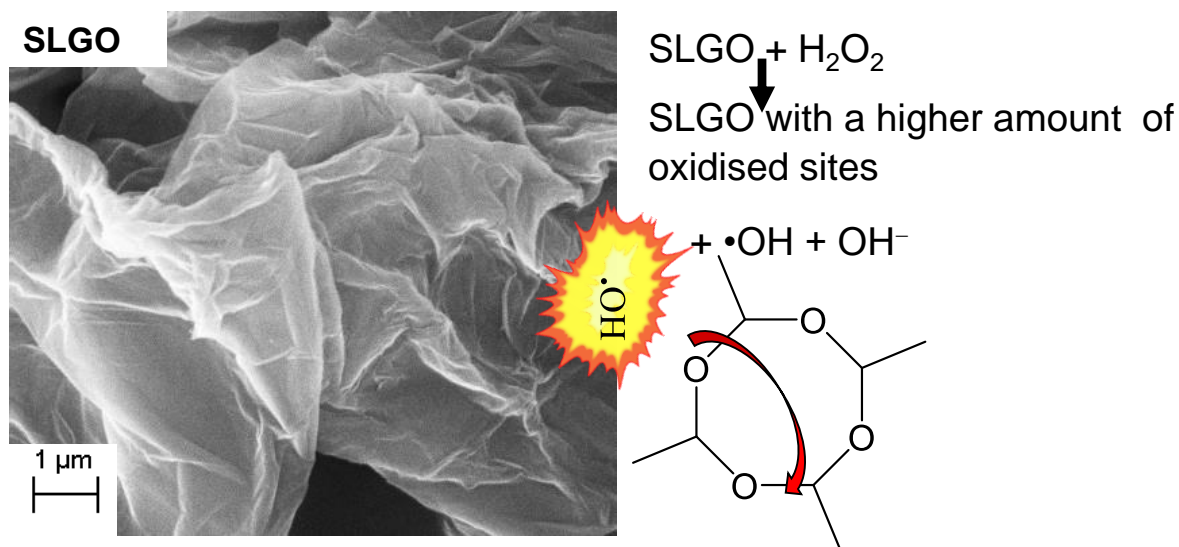
## **Abstract**

A modified graphene oxide-based Fenton's reaction has been investigated for the degradation of a challenging emerging contaminant which is not effectively removed in conventional water treatment. Metaldehyde, used as the challenge molecule in this study, is a common molluscicide that (like many highly soluble contaminants) has frequently breached European regulatory limits in surface waters. The new method involves graphene with higher hydrophilic characteristics (Single-Layer Graphene Oxide, SLGO) as a system that participates in a redox reaction with hydrogen peroxide and which can potentially stabilize the  $\bullet\text{OH}$  generated, which subsequently breaks down organic contaminants. The modified Fenton's reaction has shown to be effective in degrading metaldehyde in natural waters (>92% removal), even at high contaminant concentrations (50 mg metaldehyde/L) and in the presence of high background organic matter and dissolved salts. The reaction is relatively pH insensitive. SLGO maintained its catalytic performance over 3 treatment cycles when immobilized. Its performance gradually decreased over time, reaching around 50% of starting performance on the 10<sup>th</sup> treatment cycle. X-ray Photoelectron Spectroscopy (XPS) analysis of modifications caused in SLGO by the oxidizing treatment indicated that the oxidation of C-C  $\text{sp}^2$  to carbonyl groups may be the cause of the decrease in performance. The proposed modified Fenton's process has the potential to substitute traditional Fenton's treatment although regeneration of the nanocarbon is required for its prolonged use.

## **Highlights:**

- SLGO and  $\text{H}_2\text{O}_2$  can degrade metaldehyde-contaminated water
- pH and total organic carbon are not critical in the modified Fenton's process
- SLGO has been immobilized and can be re-used
- Regeneration of SLGO is needed to improve cost-effectiveness

**Keywords:** Single Layer Graphene Oxide (SLGO); Fenton; catalysis; water treatment; metaldehyde.



## 1. Introduction

Conventional water treatment processes show limited efficiency for a number of increasingly utilised organic chemicals, which are then discharged to the environment after their incomplete removal. As a consequence, a range of biologically-active micropollutants can be found at parts per billion level in surface and drinking waters (e.g. estrogens, personal care products, pharmaceuticals, pesticides, organic solvents, disinfection by-products)[1-3]. One example of these biologically-active micropollutants is metaldehyde, a molluscicide widely used in large-scale agriculture and in gardens, particularly in regions (such as NW Europe, South East Asia, parts of China and the USA) where long wet seasons require the control of molluscan pests. . Metaldehyde has been observed frequently to breach European regulatory limits in surface and drinking waters (0.1 μg/l, based on the European Drinking Waters Directive 1998 and 2000) [4,5] in the UK and elsewhere due to its high solubility and frequent application [6]. This highly polarmolecule is relatively resistant to conventional chlorination or ozonation treatment, and is one of a group of emerging contaminants such as acrylamide, geosimine, 1,1,1-trichloroethane, and methyl tert-butyl ether (MTBE) that (due to their small organic “skeleton”) show limited

interaction with the conventional granular activated carbons (GAC) currently applied in tertiary water treatment [7, 8]. It was reported in 2011 that water treatment works could achieve a removal of only up to 50% metaldehyde, and that the regulatory limit target was difficult to achieve [9].

Recent research into metaldehyde and similar emerging or problem contaminants has focused on developing improved adsorptive or catalytic destruction methods for their removal from treated waters. For example, Busquets *et al.* noted the improved adsorption of metaldehyde using “tailored” activated carbon beads (i.e. with controlled surface chemistry and pore size distribution) synthesised from phenolic resin [10,11], while Autin *et al.* reported successful photodegradation of metaldehyde using UV/H<sub>2</sub>O<sub>2</sub> and UV/TiO<sub>2</sub> (although the effectiveness of metaldehyde removal was significantly reduced by the presence of background organic matter) [12]. Bing and Fletcher report the destruction of metaldehyde using sulfonic acid functionalized mesoporous silica [13], and ion exchange resins with sulfonic acid groups in a system that can also adsorb any acetaldehyde generated [14], while Nabeerasool *et al.* report effective removal of metaldehyde using a coupled batch adsorption/ electrochemical regeneration technique, based on low capacity graphitic material (Arvia™ process) [8]. A slow but sustained oxidation of metaldehyde (31% degradation in 60h) was also achieved using macrocyclic ligand catalysts based on Fe(III) and H<sub>2</sub>O<sub>2</sub> (TALM/H<sub>2</sub>O<sub>2</sub>) [15].

The use of nanocarbon-based materials in adsorptive and catalytic applications for removal or destruction of emerging (or problem) contaminants has also been widely discussed [16-20]. Graphene in particular has been the focus of much research due to its high specific surface area, tunable surface behaviour, and extremely high electron mobility [21-22]. Graphene-based materials have been used as adsorbents or heterogeneous (photo)catalysts for effective removal or degradation of a range of heavy metal/metalloid and organic contaminants, including As, Cr, U, dyes, bisphenol A, perchlorate, bulk oil and gasoline [17,19, 23-25]. Graphene can also

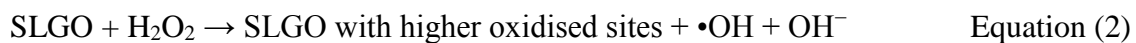
be used as part of a modified Fenton's process to generate the highly reactive and oxidizing hydroxyl radical (2.8V oxidation potential) from hydrogen peroxide, which in turn can effectively degrade a range of common organic contaminants. For example, Liu et al. used a graphene oxide-FeS<sub>2</sub> composite, in the presence of H<sub>2</sub>O<sub>2</sub>, to degrade 4-chlorophenol (97% removal within 60 min, pH 7, starting concentration of 4-chlorophenol: 128.6 mg/L) [26]. Given the hydrophobic nature of 4-chlorophenol, this contaminant could also be adsorbed in addition to being chemically degraded by the Fenton's reaction, although this mechanism was not explored in the aforementioned work. Further insights into the role of graphene oxide in Fenton's reaction processes have been given by a system where the nanomaterial was doped with Fe<sub>3</sub>O<sub>4</sub>: here Csp<sup>2</sup> was oxidised and the electrons transferred to the Fe<sub>3</sub>O<sub>4</sub>, which enhanced the catalytic efficiency [27].

The standard Fenton's process whereby iron salts activate and catalyze the decomposition of H<sub>2</sub>O<sub>2</sub> is shown in Equation (1) (for which optimal conditions are at acid pH, i.e. pH 3). Equation (2) shows an alternative, modified Fenton's process using single layer graphene oxide (SLGO) as a heterogeneous catalyst, which operates at neutral and alkaline pH [28].

"Standard" Fenton's process (Fe<sup>2+</sup>)



Modified Fenton's process using SLGO



In both reactions H<sub>2</sub>O<sub>2</sub> can act as an •OH scavenger as well as an initiator, as shown in Equation (3).



Voitko *et al.* compared the H<sub>2</sub>O<sub>2</sub> decomposition capability of various nanoscale and macroscale (activated) carbons, and observed that single layer graphene oxide (SLGO) exhibited greater reaction rate stability over repeated reaction cycles than bulk activated carbon, or N-doped, oxidized and as-supplied carbon nanotubes (CNTs) [21]. Thus, this work implied that SLGO may have potential for repeated use in water treatment applications. The potential benefits of graphene-based processes (shown in Equation (2)) over conventional Fenton processes involving an addition of ferric ions (Equation (1)) include effective catalytic performance with less need for strict pH control (as long as the pH is sufficiently stable to avoid folding and agglomeration of the graphene [29]) and easier separation of graphene (as compared to a homogenous catalyst such as cationic Fe<sup>2+</sup>) from the reaction mixture following application. In this study, we examine this modified Fenton's process in more detail, its effect on SLGO chemistry, and report for the first time the effective oxidative degradation of metaldehyde in environmental waters using a SLGO – peroxide treatment.

## **2. Materials and methods**

### **2.1 Chemicals**

Single-layer graphene oxide (SLGO) was obtained from Cheap tubes Inc. (USA). Metaldehyde (analytical grade), and 2-chloro-4-ethyl-d<sub>5</sub>-amino-6-isopropylamino-1,3,5-triazine (d<sub>5</sub>-atrazine, 99% purity, used as an internal standard) were purchased from Sigma Aldrich (UK). Metaldehyde stock solutions were prepared by dissolving the standard in 5% methanol in water and diluting further with ultrapure water, surface water or buffer solutions for the preparation of spiked aqueous samples. Some experiments used higher concentrations of metaldehyde than typical environmental levels to assess degradation processes and possible adsorption of metaldehyde onto SLGO under conditions of potential maximum adsorption. Levels of metaldehyde resembling environmental conditions (2 μg/L) were used in a kinetic study. The

conditions assayed to test the stability of metaldehyde in systems where  $\cdot\text{OH}$  was generated are given in Table 1. These conditions include use of 0.3M  $\text{Fe}^{2+}$ , which was prepared by dilution of  $\text{FeSO}_4 \cdot 7\text{H}_2\text{O}$  (from BDH Laboratory supplies, UK) (1M) in aqueous solution at 50 °C, followed by cooling to 25°C. All studies in this work were carried out at 25 °C. Ultrapure water, generated with an ELGA Purelab purification system (Veolia, UK) was used throughout the study, unless otherwise specified.

The SLGO structure (sheets of 300 nm x 800 nm and thickness of 0.7 - 1.2 nm approximately) was confirmed with Atomic Force Microscopy (AFM) by the supplier and analysis by Transmission Electron Microscopy (TEM) by our team [29,30]. Scanning electron microscopy images (SEM) of the SLGO, obtained using a JEOL 6310 Field Emission Scanning Electron Microscope (Oxford instruments, UK) operating at 25 eV, are provided in Supporting information (Figure S1 (Supporting information)). The surface chemistry of the SLGO was characterized using X-ray photoelectron spectroscopy (XPS) using methods detailed in the following section.

## **2.2 X-ray photoelectron spectroscopy (XPS)**

XPS was performed using an ESCALAB 250 Xi system (Thermo Scientific) equipped with a monochromated Al  $\text{K}\alpha$  X-ray source, a hemispherical electron energy analyzer, a magnetic lens and a video camera for viewing the analysis position. The standard analysis spot of *ca.*  $900 \times 600 \mu\text{m}^2$  was defined by the microfocused X-ray source. Full survey scans (step size 1 eV, pass energy 150 eV, dwell time 50 mS) and narrow scans (step size 0.1 eV, pass energy 20 eV, dwell time 100 mS) of the C1s (binding energy, BE  $\sim$ 285 eV), O1s (BE $\sim$ 531 eV), N1s (BE  $\sim$ 399 eV) and S2p (BE  $\sim$ 164 eV) regions were acquired from three separate areas on each sample. Data were transmission function corrected and analyzed using Thermo Avantage Software (Version 5.952) using a smart background. The XPS analysis was carried out on

washed (free or immobilized on tape) SLGO (see section 2.5) and SLGO treated with a range of doses of 1% H<sub>2</sub>O<sub>2</sub> and reaction times (specified in section 2.5) following drying in air.

### **2.3 Fourier Transform Infrared spectroscopy (FTIR)**

FTIR analysis of the nanomaterial, free and immobilized on tape (using the same samples characterized with XPS), was performed in ATR (Attenuated Total Reflectance) mode with a model 3i FTIR spectroscopy system from ThermoFisher Scientific (UK). The surface chemistry of the SLGO was characterized after letting the washed nanomaterial dry in air (washing conditions are given in 2.5).

### **2.4 Chromatography-mass spectrometry**

Metaldehyde was analysed via fast liquid chromatography coupled to mass spectrometry (LC-MS) [10]. Potential compounds arising from the degradation of metaldehyde were examined by gas chromatography-mass spectrometry with electron impact and a quadrupole analyser (GC-EI-MS, Agilent model 7890, Agilent Technologies, Santa Clara US). A BP5 fused-silica capillary column of 30m x 0.25mm I.D with 0.25µm film thickness and stationary phase 5% phenyl polysiloxane (SGE Analytical Science, UK) was used for the separation, which was carried out with He at 1ml·min<sup>-1</sup>. The injection temperature was 250°C. The oven temperature program involved 2 min at 50 °C increasing to 250 °C at a rate of 20°C/min. The injection volume was 1µl with split 1:2. The acquisition was carried out simultaneously in both Full scan (scan range *m/z* 40-200) and Single Ion Monitoring modes, the latter following the fragment ions *m/z* 89 and 45. Identification was assisted by reference to the NIST 08 standard reference database (National Institute of Standards and Technology, Gaithersburg, US). The preparation of buffer solutions and incubation conditions is described in the Supplementary Information.

### **2.5 Degradation of metaldehyde with SLGO**



Commercial SLGO was washed with ultrapure water. This involved stirring and separation by centrifugation steps (10 min, 4000 rpm, x 5) to remove impurities from its preparation before its use in batch studies. In studies involving SLGO immobilized onto tape, the nanomaterial was washed by immersing the immobilised SLGO in water (stirred for ca. 10 min, 5 changes of water) before its use. SLGO had been immobilised by dispersing it onto conventional cellulose tape, obtained from a local store, with the help of a spatula. Subsequently, a strip of tape was put on the top of the strip with SLGO in a sandwich-like configuration, and both strips were pulled apart to obtain a thinner layer of SLGO, resulting in (0.13 mg SLGO/cm tape). Batch conditions used SLGO immobilized onto cellulose tape (15 cm), which was rolled, placed onto a flask interior wall (see Figure S2 (Supporting information)) and washed, as indicated in 2.5, which allowed removal of impurities and separation of non immobilized SLGO. Metaldehyde was added to water or buffer (20 mL) poured into the flask, which covered the immobilized SLGO. The reaction started when H<sub>2</sub>O<sub>2</sub> (0.2mL) was added in solution, which was magnetically stirred. Conditions used for reaction of non immobilized SLGO with metaldehyde in buffered systems, at different concentrations of SLGO and FeSO<sub>4</sub>, are given in Table 1.

Kinetic studies followed the same set up as the system described with immobilized SLGO and samples (0.2ml) were taken at the following time points: 0, 5, 15, 30, 40, 60, 90 min and 12, 16 h. The kinetic studies were carried out at starting concentrations of 31 mg metaldehyde/L and 2 $\mu$ g metaldehyde/L. The concentration of metaldehyde with time was adjusted to first and second order rate equations, linearised expressions for which are given in (1) and (2) respectively. In these expressions,  $k$  is the velocity constant of the reaction and the starting and instantaneous concentrations of metaldehyde are expressed as [metaldehyde]<sub>0</sub> and [metaldehyde], respectively.

$$\ln[\text{metaldehyde}] = \ln[\text{metaldehyde}]_0 - k t \quad \text{Equation (4)}$$

$$\frac{1}{[\text{metaldehyde}]} = \frac{1}{[\text{metaldehyde}]_0} + k t \quad \text{Equation (5)}$$

## 2.6 Characterisation of water samples

Surface and tap water samples were analyzed for total carbon (TC) and total inorganic carbon (TIC) with a Shimadzu TOC-V CSH/CSN (Kyoto, Japan). Samples were filtered through glass wool and frozen until analysis. Hydrochloric acid (2M) was used for the determination of TIC. Total organic carbon (TOC) was determined by the difference between TC and TIC. For the TC and TIC analysis, glassware was rinsed with 1% HCl in ultrapure water, then washed with acetone and dried before use. The analyses were carried out in triplicate and blanks were run between samples.

## 2.7 Data analysis

Statistical treatment: t-student significance tests and two way ANOVA factorial analysis, which was carried out with Minitab software version 16.0, were used to assess the effect of three pairs of three parameters on the degradation of spiked metaldehyde in water.

The interaction of metaldehyde in aqueous solution with graphene was modeled using MMFF94 force field minimisation molecular dynamics with ChemBio3D ultra 14.0 (from PerkinElmer, UK) using 5000 iterations. Graphene was simulated as a planar sheet made of 16

benzenes incorporating 6 hydroxyl groups and a carboxylic acid located at its edges. The behavior of the model was studied in aqueous solution at 298 K.

### **3. Results and discussion**

#### **3.1 Individual effect of SLGO and H<sub>2</sub>O<sub>2</sub> on metaldehyde**

Batch studies were performed to assess the individual effect of H<sub>2</sub>O<sub>2</sub> and SLGO on metaldehyde between pH 3 and 12. It has been reported that metaldehyde can be depolymerized by strong acids [13, 31] and so a decrease in metaldehyde concentration observed at pH 3, in the absence of SLGO, is an effect of chemical degradation (Figure S3 (Supporting information)). The addition of suspended SLGO, even at concentrations as high as 375 mg SLGO/L, did not cause observable removal of metaldehyde by adsorption within the studied pH range (P 0.05) (Figure S3 (Supporting information)). A model illustrating the interaction between metaldehyde and SLGO in aqueous solution was constructed using MMF94 force field minimization and molecular dynamics (Figure S4 (Supporting information)) which confirmed the tendency of metaldehyde not to adsorb onto SLGO in aqueous solution. Further discussion and interpretation of this model can be found in Supporting information S2. The individual effect of H<sub>2</sub>O<sub>2</sub> on metaldehyde was initially studied, at 0, 1, 5 and 10% H<sub>2</sub>O<sub>2</sub> at pH 8.5 (pH adjusted with 0.5M NaOH), without SLGO addition and with a reaction time of 35 mins. This pH was chosen to favor the suspension of SLGO in solution [30], as well as the generation of •OH [28] (although the disproportionation of H<sub>2</sub>O<sub>2</sub> also takes place at this pH). The maximum degradation of metaldehyde observed (20%) occurred with 1% H<sub>2</sub>O<sub>2</sub> and did not increase when the proportion of the oxidant was increased (Figure S5). When SLGO (100mg SLGO/L) was added to the solution under the same conditions (i.e. with 35 min reaction time and at pH 8.5,

with 1% H<sub>2</sub>O<sub>2</sub>), 76.0 ± 3.4 % of metaldehyde was decomposed (12 mg metaldehyde/L remained in solution from the starting 50 mg/L of metaldehyde, n=3), which indicates an enhancement of the generation of radical species or their more effective action due to interaction with SLGO. This degradation was not enhanced when repeating the experiment but adding 5% H<sub>2</sub>O<sub>2</sub> (data not shown) which indicated that H<sub>2</sub>O<sub>2</sub> was in excess.

Earlier work found that CNTs (which could be described as a rolled sp<sup>2</sup> graphene layer), when in suspension, could scavenge •OH [32]. Hydroxyl radical species could potentially gain some stability in the graphene electronic cloud which would increase their lifespan (analogous to other systems where hydroxyl radical stability can be increased by π –bond interaction, such as with α-tocopherol (vitamin E)) and so their potential to react with organic molecules approaching the suspended graphene surface.

### **3.2 Synergy between pH, SLGO and Fe<sup>2+</sup> in the degradation of metaldehyde**

Following assessment of the individual and combined roles of SLGO and H<sub>2</sub>O<sub>2</sub> in the degradation of metaldehyde, the efficacy of the SLGO and Fe<sup>2+</sup>-based Fenton's processes was compared at constant H<sub>2</sub>O<sub>2</sub> initial concentration and varying pH levels, in a 2<sup>3</sup> experiment designed as shown in Table 1. Reaction pH was controlled by buffer solutions (100mM acetic acid/ammonium acetate for pH 5, and 100 mM ammonia/ammonium acetate for pH 8.5) in every experiment. The pH in buffered systems remained stable during the experiment. In contrast, the pH evolved to 2 in non-buffered systems containing Fe<sup>2+</sup> where the initial media was adjusted with 0.5M NaOH or 0.5M HCl, leading to degradation of metaldehyde. While metaldehyde is effectively removed at pH 2, such low pH conditions are unsuitable for large scale water treatment due to a requirement for post-treatment alkalization.

Hydrogen peroxide, H<sub>2</sub>O<sub>2</sub> (without Fe<sup>2+</sup> or SLGO addition, condition 1, Figure 1) was more effective in degrading metaldehyde at alkaline pH 8.5. The increase in the reaction time with

respect to the conditions initially assayed in section 3.1 (i.e. from 35 to 60 minutes) tripled the degradation of metaldehyde. Systems with SLGO enhanced the metaldehyde degradation process (condition 2, Figure 1). The reduction of metaldehyde in solution was solely through catalytic degradation as adsorption onto SLGO was found not to occur (section 3.1) and metaldehyde was chemically stable at the pH assayed. In Figure 1, the catalytic effect of SLGO at the 2 different pHs assayed was not found to differ ( $P < 0.05$ , condition 2), despite the expected different conformations of SLGO in suspension at these pHs [30], which might have affected the catalytic activity. Notably, since achieving degradation of contaminants without addition of  $\text{Fe}^{2+}$  has high economic and environmental relevance in water treatment, the system with SLGO (condition 2, Figure 1) was found to be as effective as the system with  $\text{Fe}^{2+}$  (condition 3, Figure 1) at enhancing the degradation of metaldehyde.. Similar performance was observed in a system with combined  $\text{Fe}^{2+}$  and SLGO (condition 4, Figure 1). In these three conditions (2, 3 and 4), the degradation of metaldehyde was found to be complete (i.e. not significantly different to 100%) at pH 5 ( $P < 0.05$ ). No statistical difference was found between performance under the conditions assayed in conditions 2 - 4, and the pH did not significantly affect metaldehyde degradation ( $P < 0.05$ ) (conditions 2-4), although there is a general tendency for slightly reduced degradation at higher pH (pH 8.5). The performance achieved with condition 1 was significantly lower ( $P < 0.05$ ) than with conditions 2-4.

The weight ratio  $\text{Fe}^{2+}/\text{SLGO}$  used in the study was 167 and the molar ratio  $\text{Fe}^{2+}/\text{H}_2\text{O}_2$  was 1:1. Every mole of  $\text{Fe}^{2+}$  could potentially be oxidised by  $\text{H}_2\text{O}_2$  and generate  $\bullet\text{OH}$ , whereas only some functional groups on SLGO (i.e. phenolic alcohols: 2.39 mmol/g) could. We estimate that the molar  $\text{Fe}^{2+}/\text{phenolic OH}$  in SLGO ratio was in the region of 418 in our system, which was expected to result in less degradation of metaldehyde by SLGO than with  $\text{Fe}^{2+}$  if they had the same redox potential. In fact, similar results were observed for both components, indicating

that the system tended to be  $\text{H}_2\text{O}_2$  limited rather than being limited by the number of oxidisable sites on the SLGO.

The relation between the three factors pH,  $\text{Fe}^{2+}$  and SLGO was analyzed by factorial analysis in order to confirm their impact on the degradation of metaldehyde. In an interaction plot of results from the statistical analysis (Figure 2), parallel lines indicate no interaction between the variables, and the greater the difference in slope between the lines the greater the degree of interaction. A strong interaction was found between pH and SLGO as well as pH and  $\text{Fe}^{2+}$  on the concentration of metaldehyde in solution. In contrast, the interaction between SLGO and the concentration of  $\text{Fe}^{2+}$  was not found to enhance the degradation process.  $\text{Fe}^{2+}$  or SLGO, which can become oxidized in the presence of  $\text{H}_2\text{O}_2$ , did not appear to interact with each other, which would have led indirectly to a decrease in the degradation of metaldehyde. This indicates that traditional Fenton's reaction and the modifications presented in this study could potentially co-exist in wastewater tertiary treatment. The dependency of the degradation of metaldehyde on the concentration of graphene oxide and an estimate of the concentration of SLGO required for treating environmentally realistic concentrations of the molluscicide has been included in supporting information S3 and Figure S6 (Supporting information).

### **3.3 Degradation of metaldehyde in spiked surface water samples with suspended SLGO and $\text{H}_2\text{O}_2$**

The degradation of contaminants by heterogeneous catalysis can be significantly affected by the presence of other components in the aqueous medium. For an instance, the degradation of metaldehyde by photocatalysis using nano- $\text{TiO}_2$  was observed to be greatly inhibited in natural waters compared to deionised water, possibly due to the adsorption of organic matter onto the catalyst's active sites [13]. To test the robustness of the degradation of metaldehyde with SLGO/ $\text{H}_2\text{O}_2$ , a range of natural waters (and tap water) were incubated in batch mode with

SLGO and 1% H<sub>2</sub>O<sub>2</sub>. Our previous data indicated that pH 5 and 8.5 could provide satisfactory degradation of metaldehyde (Figure 1). Hence, the pH of the surface water samples was not adjusted for the experiment. Indeed, the pH of the water samples tested (pH 6.7-8.3) favored the suspension of SLGO in water [30]. Specifically, the waters used were: tap water (Brighton, Sussex, UK, pH 7.9, TOC 3.6 mg/L); lake water (Balcombe, Sussex, UK, pH 7.8, TOC 6.2 mg/L); reservoir water (Ardingly, Sussex, UK, pH 8.1, TOC 7.6 mg/L); river water (Ouse river, Spatham Lane, Sussex, UK, pH 8.3, TOC 10.3 mg/L); and estuarine (i.e. brackish) water (Newhaven, Sussex, UK, pH 8.1, TOC 6.7 mg/L).

The degradation of metaldehyde obtained (Figure 3) indicates that the heterogeneous catalysis by SLGO/H<sub>2</sub>O<sub>2</sub> was not affected significantly by varying TOC and background salts content (P 0.05). The mean degradation efficiency, which was above 94%, was not lower than the efficiency obtained for spiked deionised water (condition 2, Figure 1), possibly because of the limited adsorptive capacity of SLGO for dissolved organic matter, or that the degradation of metaldehyde took place before the active sites of SLGO became unavailable.

### **3.4 Immobilisation of SLGO onto cellulose tape and an assessment of the repeatability of metaldehyde degradation**

Uncertainties over the toxicology of SLGO and its high cost discourage the application of suspended SLGO in large scale water treatment. For that reason, the degradative performance of SLGO/H<sub>2</sub>O<sub>2</sub> was tested with SLGO in an immobilized state, i.e. surface bound on a fine layer of cellulose tape (as shown in Figure 4 and in further experimental information discussed in section 2). The catalytic degradation of metaldehyde (spiked at 26 mg/L in ultrapure water) with 1% H<sub>2</sub>O<sub>2</sub> was investigated over several cycles at pH 5 (adjusted with NaOH) and at the pH of the initial water sample (pH 8). SLGO maintained its degradative performance when

surface immobilized although the change in capacity for metaldehyde degradation over repeat cycles was significant (Figure 4); the degradation was stable for 3 cycles after which it dropped by 30%, and on the 10<sup>th</sup> cycle the performance was about 50% of the starting performance. This result is compatible with a slight decrease in the decomposition of H<sub>2</sub>O<sub>2</sub> caused by SLGO on a 10<sup>th</sup> treatment cycle observed in previous work [21]. SEM was used to examine the starting SLGO and the SLGO immobilised on cellulose tape which had been used in 1 and 10 treatment cycles, but no qualitative differences in surface characteristics were observed (Fig S1). XPS and FTIR analysis of the same samples however did identify chemical changes occurring on the surface of the SLGO. XPS analysis showed that in all SLGO samples, a comparatively small amount of carboxyl groups and high amounts of hydroxyl and carbonyl groups were observed (Table 2). Example C1s de-convoluted narrow scan spectra [33] are shown in Figure 5. A single oxidation step with H<sub>2</sub>O<sub>2</sub> led to a significant change in the C/O ratio as shown in Table 3. A decrease in ratio of ca. 40% was caused by an increase in carbonyl groups (C=O) (Table 2 and Figure 5). The increase in carbonyl groups was also associated with a decrease in sp<sup>2</sup> hybridized carbons. This phenomenon of changes in the sp<sup>2</sup> carbon is in agreement with findings by Xing et al. [34] who noted gradual structural degradation of graphene under H<sub>2</sub>O<sub>2</sub> attack, due to destruction of C-C bonds around defect sites. The oxidation degree (C/O ratio), and the abundance of alcohol/ether (C-O) and hydrocarbon contributions, did not significantly change after ten treatments with H<sub>2</sub>O<sub>2</sub>. However the carbonyl (C=O) contribution increased by 25% to 30% after the tenth oxidising step, although the sp<sup>2</sup> hybridized carbon remained unchanged. This increase in stable carbonyl bond formation could have caused the decrease in performance observed particularly after the third oxidising treatment (Figure 5). Measures are required therefore to preserve the sp<sup>2</sup> hybridized carbon and reduce the increase in C=O bonds formation in order to make the use of SLGO viable economically and technically in this modified Fenton's process. The FTIR analysis of the samples was in agreement with the XPS



results. The intensity of the bands at 1730 and 1230  $\text{cm}^{-1}$ , corresponding to stretching of carbonyls C=O and C-O groups, respectively, changed with the oxidising treatment with 1%  $\text{H}_2\text{O}_2$  (shown in Figure S5 (Supporting information)). The C=O band increased its intensity mainly with the first treatment, and less increase was observed after the 10<sup>th</sup> oxidising treatment. The increases in the 1730  $\text{cm}^{-1}$  band indicates higher abundance of groups containing C=O, which can be esthers, ketones, aldehydes or carboxylic acids. Unlike the XPS scan, the FTIR data did not offer enough resolution to distinguish the origin of the vibration between C=O and O=C-O, and therefore XPS data is preferred for the interpretation of the results. The FTIR data were less sensitive to changes in C-O (slight increase observed with oxidizing treatments) and did not detect strong changes in C=C bands (1630 and 1425  $\text{cm}^{-1}$ ) or the  $\text{Csp}^2$ -H and  $\text{Csp}^3$ -H band stretches at around 2900-3000  $\text{cm}^{-1}$  as a result of the treatment (Figure S7(Supporting information)).

### **3.5 Kinetic study on the degradation of metaldehyde with immobilised SLGO and assessment of degradation products.**

The concentration of metaldehyde decreased in solution after the application of a single dose of  $\text{H}_2\text{O}_2$  (1%) in a stirred system with immobilised SLGO (Figure 6). When the starting concentration of metaldehyde was 31 mg/L, its concentration decreased for the first 90 minutes and was found to be stable thereafter. The decrease of metaldehyde concentration in solution over time did not fit to a first order reaction kinetic (1) but instead followed a second order reaction (Figure 6). The constant of the reaction was 0.0041  $\text{l}\cdot\text{mg metaldehyde}^{-1}\cdot\text{min}^{-1}$  ( $12\text{ M}^{-1}\cdot\text{s}^{-1}$ ) which is a much slower reaction than the photocatalytic process with UV/ $\text{TiO}_2$  reported by Autin et al. [12], with a reaction rate of  $1.3\cdot 10^9\text{ M}^{-1}\cdot\text{s}^{-1}$  in ultrapure water. When an environmentally realistic starting concentration of 2 $\mu\text{g metaldehyde/L}$  was treated under the

same experimental conditions, the level of the molluscicide similarly decreased, although this could only be monitored for the first 25 minutes (after which the concentration of metaldehyde reached the limit of quantification of the determination ( $0.3\mu\text{g/L}$ )). A volatile degradation product of metaldehyde could be detected with GC-MS at reaction times between 15 and 30 minutes. The peak of this degradation product had a retention time of 3.34 min and the base peak of the full scan spectra was  $m/z$  45 (Figure 7). At a lower scan range, the base peak was  $m/z$  31 but the background noise was high in that  $m/z$  region as oxygen presents a signal in close proximity. The NIST library indicated that the degradation product detected was most likely hydroxyl acetic acid (also called glycolic acid), which would have resulted from opening of the metaldehyde ring and further oxidation of the methyl group in metaldehyde. Glycolic acid is used to acidify food products which denotes that it is not a toxic product [34]. The presence of other possible degradation products, such as acetic acid, acetaldehyde and ethyl acetate was examined using full scan mode. The base peaks in the mass spectra for these compounds in electron impact were  $m/z$  43 for acetic acid and ethyl acetate; and  $m/z$  44 acetaldehyde, respectively in the working conditions, and were not detected in the samples. Earlier work developing methods for the oxidation of metaldehyde has reported the production of acetic acid and acetaldehyde with TALM catalysis/ $\text{H}_2\text{O}_2$  [15]; and acetaldehyde with mesoporous silica functionalized with sulphonic acid [13]; although no degradation products were observed with the graphite based adsorbent Nyex<sup>TM</sup> and electrochemical regeneration [8] suggesting complete degradation of the molluscicide to  $\text{CO}_2$  in this system. Degradation products were not detected during metaldehyde photocatalysis with UV/ $\text{TiO}_2$  [12], although volatile by-products in this system, if present, would probably have been lost during the sample treatment carried out, which involving sample pre-concentration with styrene divinylbenzene cartridges. This is because of the high volatility of the possible degradation products and limited adsorption onto the stationary phase due to the short hydrocarbon skeleton of the

possible degradation products. In the current study, the degradation product identified as hydroxyl acetic acid was not detected at longer reaction times, presumably because it volatilised in the stirring system. LC-MS analysis in full scan mode did not show any newly generated ionic species as a result of the degradation. The toxic metaldehyde degradation monomer unit acetaldehyde was not detected, indicating rapid oxidation to volatile (non toxic) degradation product(s) and CO<sub>2</sub>.

## **Conclusions**

Effective degradation of the highly polar (and currently problematic, from the point of view of its resistance to conventional waste water treatment) contaminant metaldehyde in a range of natural waters (without pH adjustment or addition of iron salts) was observed using immobilized SLGO and 1% H<sub>2</sub>O<sub>2</sub> in a modified Fenton's process. The modified Fenton's process generates •OH which (based on degradation product analysis) breaks metaldehyde's ring structure and causes further oxidation to hydroxyl acetic acid and CO<sub>2</sub>. This shows the possibility to (a) effectively remove metaldehyde from treated water via heterogeneous catalysis processes, and (b) substitute the widely applied conventional Fenton process with potentially "greener" (in terms of reduced Fe salts use, reduced need for pH control, and easier post-treatment separation) and more effective nano-based heterogeneous catalytic treatment. Further studies however are required to address structural degradation and reduction in reactivity induced in SLGO by repeated H<sub>2</sub>O<sub>2</sub> attack, sustainable ways to regenerate the catalyst to increase its lifespan, and ways to overcome mass transfer limitations, which are inherent in the use of nanomaterials for the treatment of high volumes of water in drinking and wastewater treatment facilities.

## Acknowledgements

This work was supported by the EC Seventh Framework Programme Marie Curie Actions.

The Intra European Fellowship (Polarclean, project no. 274985) is acknowledged for financial support. The authors are grateful to Dr. Raymond L.D. Whitby for advice on the performance of SLGO. Richard Giddens is acknowledged for assistance with SEM.

## References

- [1] B. Petrie, R. Barden, B. Kasprzyk-Hordern, A review on emerging contaminants in wastewaters and the environment: current knowledge, understudied areas and recommendations for future monitoring, *Water Res.* 72 (2015) 3-27.
- [2] S.D. Richardson, T.A. Termes, Water analysis: emerging contaminants and current issues, *Anal. Chem.* 48 (2014) 2813-2848.
- [3] J.L.Schnoor, Re-Emergence of Emerging Contaminants, *Environ. Sci. Technol.* 48 (2014) 11019-11020.
- [4] Council of the European Communities, Directive of the European Parliament and of the Council on the Quality of Water Intended for Human Consumption (98/83/EC), 1998.
- [5] Council of the European Communities, Directive of the European Parliament and of the Council Establishing a Framework for Community Action in the Field of Water Policy (2000/60/EC), 2000.
- [6] *Water UK* Website. Briefing Paper on Metaldehyde 2013; [www.water.org.uk/publications/policy-briefings/metaldehyde](http://www.water.org.uk/publications/policy-briefings/metaldehyde) (accessed 19.06.16).
- [7] M. E. Stuart, K. Manamsa, J. C. Talbot, E. J. Crane, Emerging contaminants in groundwater. British Geological Survey Open Report, OR/11/013 , <http://nora.nerc.ac.uk/14557/1/OR11013.pdf>, 123 pp., 2011 (accessed 19.06.16).
- [8] M. A. Nabeerasool, A. K. Campen, D. A. Polya, Nigel W. Brown, B. E. van Dongen, Removal of metaldehyde from water using a novel coupled adsorption and electrochemical destruction technique, *Water* 7 (2015) 3057-3071.
- [9] T, Hall, B. Holden, J. Haley. Treatment for metaldehyde and other problem pesticides. 4<sup>th</sup> Developments in Water Treatment and Supply Conference, Cheltenham, June 2011.

- [10] R. Busquets, O. P. Kozynchenko, R. L. D. Whitby, S. R. Tennison, A. B. Cundy, Phenolic carbon tailored for the removal of polar organic contaminants from water: a solution to the metaldehyde problem?, *Water Res.* 61 (2014) 46-56.
- [11] S.R. Tennison, O. P. Kozynchenko, A.B. Cundy; R. Busquets, Carbon materials and their use, WO2014080230 A1, 2014.
- [12] O. Autin, J. Hart, P. Jarvis, J. MacAdam, S. A. Parsons, B. Jefferson, Comparison of UV/H<sub>2</sub>O<sub>2</sub> and UV/TiO<sub>2</sub> for the degradation of metaldehyde: kinetics and the impact of background organics, *Water Res.* 46 (2012) 5655-5662.
- [13] T. Bing, A. J. Fletcher, Catalytic degradation and adsorption of metaldehyde from drinking water by functionalized mesoporous silicas and ion-exchange resin, *Sep. Purif. Technol.* 124 (2014) 195-200.
- [14] T. Bing, A. J. Fletcher, Development of a novel dual-stage method for metaldehyde removal from water. *Chem. Eng. J.* 284 (2016) 741-749.
- [15] L.L.Tang, M.A. DeNardo, C.Gayathri, R.R.Gil, R.Kanda,T.J. Collins, TAML/H<sub>2</sub>O<sub>2</sub> oxidative degradation of metaldehyde: pursuing better water treatment for the most persistent pollutants, *Environ. Sci. Technol.* 50 (2016) 5261–5268.
- [16] S. Ragan, R. L. D. Whitby, A. B. Cundy, Old and new carbons for wastewater treatment, *Water and Sewerage* 3 (2012) 34-35.
- [17] H. Wang, X. Yuan, Y. Wu, H. Huang, X. Peng, G. Zeng, H. Zhong, J. Liang, M. Ren, Graphene-based materials: fabrication, characterization and application for the decontamination of wastewater and wastegas and hydrogen storage/generation, *Adv. Colloid Interface Sci.* 19-40 (2013) 195-196.
- [18] S. Chae, E. Hotze, A. Badireddy, S. Lin, J. Kim, M. Wiesner, Environmental implications and applications of carbon nanomaterials in water treatment, *Water Sci. Technol.* 67 (2013) 2582-2586.
- [19] K. C. Kemp, H. Seema, M. Saleh, N. H. Le, K. Mahesh, V. Chandra; K. S. Kim, Environmental applications using graphene composites: water remediation and gas adsorption, *Nanoscale* 5 (2013) 3149-3171.
- [20] G. Ghasemzadeh, M. Momenpour, F. Omid, M. R. Hosseini, M. Ahani, A. Barzegar, *Front. Environ. Sci. Eng.* 8 (2014) 471-482.
- [21] K. V. Voitko, R. L. D. Whitby, V. M. Gun'ko, O. M. Bakalinska, M. T. Kartel, K. Laszłó, A. B. Cundy, S. V. Mikhalovsky, Morphological and chemical features of nano and macroscale carbons affecting hydrogen peroxide decomposition in aqueous media, *J. Colloid Interface Sci.* 361 (2011) 129-136.

- [22] Z. Niu, L. Liu, L. Zhang, X. Chen, Porous graphene materials for water remediation, *Small* 10 (2014) 3434-3441.
- [23] G. Ramesha, A. Kumara, H. Muralidhara, S. Sampath, Graphene and graphene oxide as effective adsorbents toward anionic and cationic dyes, *J Colloid Interface Sci.* 361 (2011) 270-277.
- [24] S. Zhang, Y. Shao, J. Liu, I. A. Aksay, Y. Lin, Graphene–polypyrrole nanocomposite as a highly efficient and low cost electrically switched ion exchanger for removing  $\text{ClO}_4^-$  from wastewater, *ACS Appl. Mater. Interfaces* 3 (2011) 3633-3637.
- [25] S. Wang, H. Sun, H. M. Ang, M. O. Tadé, Adsorptive remediation of environmental pollutants using novel graphene-based nanomaterials, *Chem. Eng. J.* 226 (2013) 336-347.
- [26] W. Liu, L. Xu, X. Li, C. Shen, S. Rashid, Y. Wen, W. Liu, X. Wu, High-dispersive  $\text{FeS}_2$  on graphene oxide for effective degradation of 4-chlorophenol, *RSC Adv.* 5 (2015) 5, 2449–2456.
- [27] N. A. Zubir, C. Yacou, J. Motuzas, X. Zhang, X. S. Zhao, J. C. Diniz da Costa, The sacrificial role of graphene oxide in stabilising a Fenton-like catalyst  $\text{GO-Fe}_3\text{O}_4$ , *Chem. Commun.*, 51 (2015) 9291-9293.
- [28] K. Voitko, A. Tóth, E. Demianenko, G. Dobos, B. Berke, O. Bakalinska, A. Grebenyuk, E. Tombácz, V. Kuts, Y. Tarasenko, M. Kartel, K. László, Catalytic performance of carbon nanotubes in  $\text{H}_2\text{O}_2$  decomposition: experimental and quantum chemical study, *J. Colloid Interface Sci.* 437 (2015) 283-290.
- [29] R. L. D. Whitby, A. Korobeinyk, V. M. Gun'ko, R. Busquets, A. B. Cundy, K. László, J. Skubiszewska-Zięba, R. Leboda, E. Tombacz, I. Y. Toth, K. Kovacs, S. V. Mikhalovsky, pH-driven physicochemical conformational changes of single-layer graphene oxide, *Chem. Commun.* 47 (2011) 9645-9647.
- [30] R. L. D. Whitby, V. M. Gun'ko, A. Korobeinyk, R. Busquets, A. B. Cundy, K. László, J. Skubiszewska-Zięba, R. Leboda, E. Tombacz, I. Y. Toth, K. Kovacs, S. V. Mikhalovsky, Driving forces of conformational changes in single-layer graphene oxide, *ACS Nano.* 6 (2012) 3967-3973
- [31] M. B. Smith, J. March, *March's Advanced Organic Chemistry: Reactions, Mechanisms, and Structure*, John Wiley & Sons, New York, 2007.
- [32] I. Fenoglio, M. Tomatis, D. Lison, J. Muller, A. Fonseca, J. Nagy, B. Fubini, Reactivity of carbon nanotubes: free radical generation or scavenging activity?, *Free Radic. Biol. Med.* 40 (2006) 1227-1233.

- [33] S. Ray, A. G. Shard, Quantitative Analysis of Adsorbed Proteins by X-ray Photoelectron Spectroscopy, *Anal. Chem.* 83 (2011) 8659–8666.
- [34] W. Xing, G. Lalwani, I. Rusakova, B Sitharaman. Degradation of graphene by hydrogen peroxide, *Part. Part. Syst. Charact.* 31 (2014) 745-750.
- [35] J. van Krieken, E. Bontenbal, Controlled acidification of food products using lactic- or glycolic acid oligomers/derivatives. *Official Gazette of the United States Patent and Trademark Office Patents*, 2013.US 08486480.

**Table 1.** Experimental conditions used in the degradation of metaldehyde (section 3.2). H<sub>2</sub>O<sub>2</sub> (1%) was added in all samples. Reaction time (60 minutes) and shaking (25°C, 90 rpm) were kept constant.

Conditions	pH	Fe <sup>2+</sup> (M)	SLGO (mg/L)
1	5.0	0	0
2	5.0	0	100
3	5.0	0.3	0
4	5.0	0.3	100
5	8.5	0	0
6	8.5	0	100
7	8.5	0.3	0
8	8.5	0.3	100

**Table 2.** XPS C1s narrow scan peak de-convolution showing available surface functional groups in SLGO immobilized on control tape (CT) and after 1 and 10 treatments with H<sub>2</sub>O<sub>2</sub> (1%).

Peak Assignments	C-C (sp <sup>2</sup> )	C-C (sp <sup>3</sup> )	C-O Alcohol/Ether	C=O Carbonyl	O=C-O Carboxylic acid
Peak BE	~284.4 eV	~285 eV	~286.4 eV	~287.3 eV	~288.8 eV
Control Tape (CT)	0	76.0 ± 0.2	15.2 ± 0.1	0	8.8 ± 0.2
CT + SLGO	10.9 ± 2.1	62.3 ± 4.3	11.3 ± 2.2	6.6 ± 1.9	8.9 ± 0.2
CT + SLGO + (1x)H <sub>2</sub> O <sub>2</sub>	5.5 ± 0.5	57.7 ± 3.3	10.6 ± 1.5	17.3 ± 1.3	8.9 ± 1.0
CT + SLGO + (10x)H <sub>2</sub> O <sub>2</sub>	6.9 ± 1.7	53.5 ± 3.9	9.3 ± 1.6	22.0 ± 3.6	8.2 ± 0.4



**Table 3.** Carbon/ oxygen (C/O) ratio measured with XPS in immobilized SLGO under no treatment with H<sub>2</sub>O<sub>2</sub> (1%), and x1 and x10 treatments with the oxidizing agent. The support (cellulose tape) has also been analysed and taken as a control.

Peak assignment	C/ O
Control Tape (CT)	5.40
CT + Single Layer Graphene oxide (SLGO)	5.07
CT + SLGO + (1x)H <sub>2</sub> O <sub>2</sub>	3.32
CT + SLGO + (10x)H <sub>2</sub> O <sub>2</sub>	3.15

**Figure 1.** Removal of metaldehyde from aqueous solution with pH control. Metaldehyde was at 25mg/L, pH was adjusted at 8.5 with 100 mM ammonium acetate/ ammonia, and at pH 5.0 with 100 mM ammonium acetate/acetic acid buffer solutions (10 ml reaction volume). All solutions containing 1% H<sub>2</sub>O<sub>2</sub> were shaken (orbital shaker at 90 rpm, 25 °C) for 60 minutes. Error bars correspond to the standard deviation from n=3.

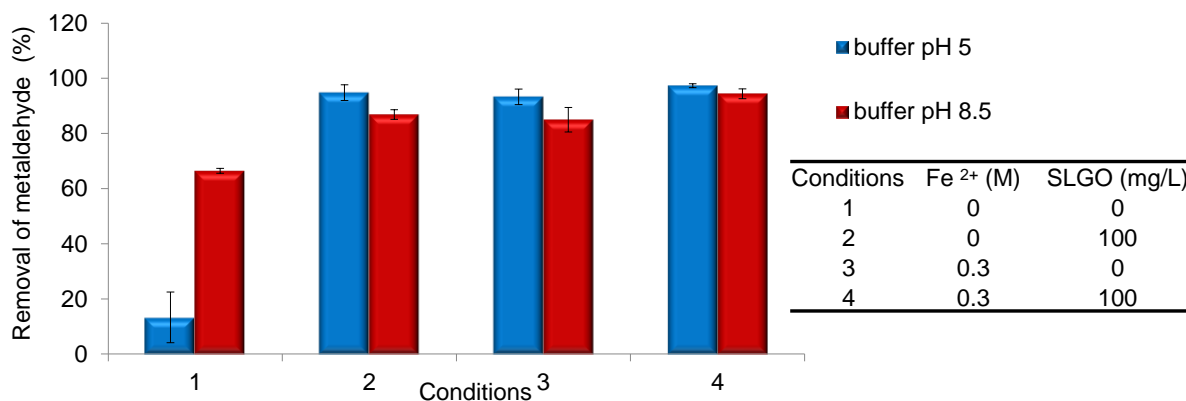


**Figure 2.** Interaction plot displaying the relationship between pH, Fe<sup>2+</sup> and SLGO. Metaldehyde degradation acts as a response variable.

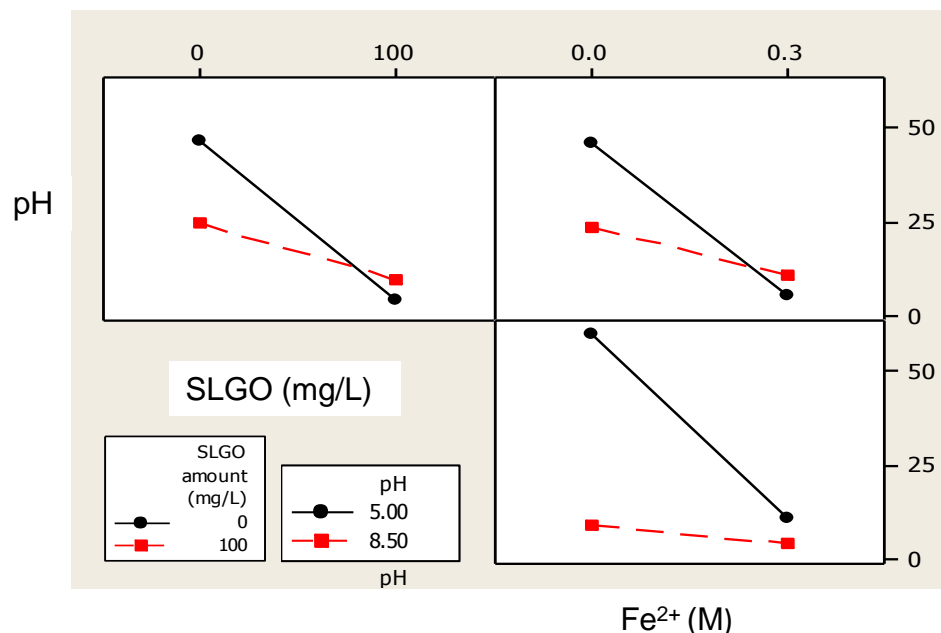


**Figure 3.** Degradation of metaldehyde in spiked tap and natural waters (spiked at 26 mg/L) using SLGO/H<sub>2</sub>O<sub>2</sub> without pH adjustment or pH buffering. (0.004 mg SLGO: 4.95 mL water: 0.05 mL H<sub>2</sub>O<sub>2</sub>). Reaction time was 60 minutes. Error bars correspond to the standard deviation from n = 3 experiments. See text for details of sampling locations (x-axis labels).

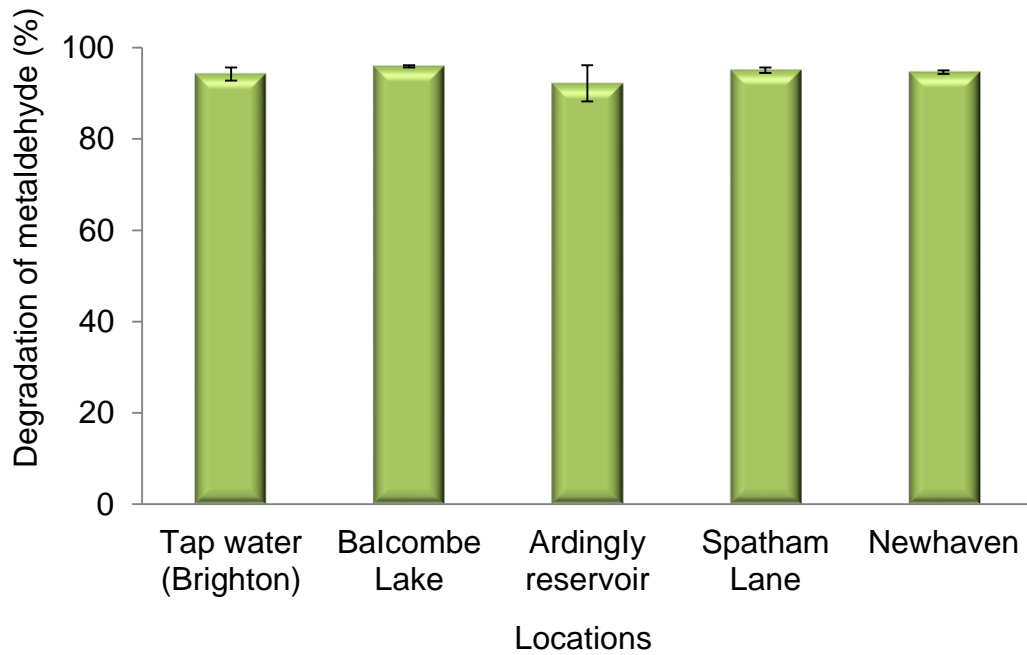


**Figure 4** Degradation of metaldehyde by immobilised SLGO (shown) and H<sub>2</sub>O<sub>2</sub> (1%) in batch mode over 10 reaction cycles (n=1). Reaction time = 60 minutes.

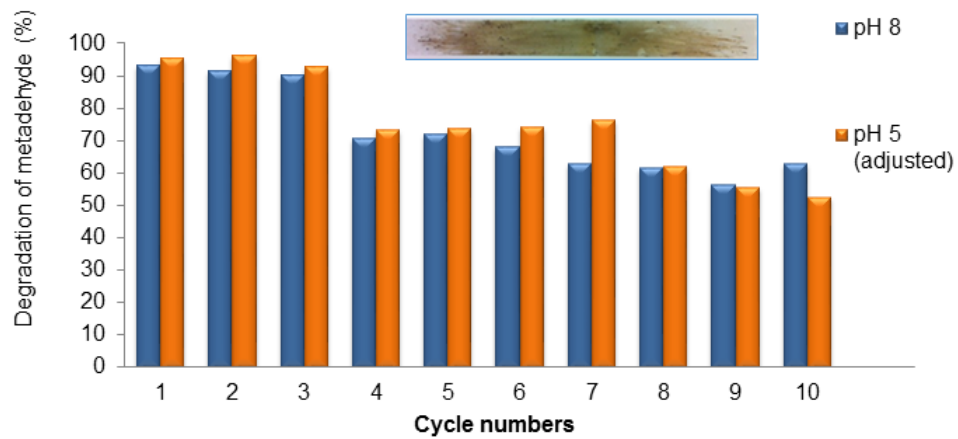


**Figure 5.** Effect of oxidizing treatments on the SLGO surface chemistry. XPS C1s narrow scan spectra of (a) Support Tape, (b) Support Tape with SLGO and (c & d) are treated with H<sub>2</sub>O<sub>2</sub> one and ten times respectively. C1s peak de-convolution is also shown on each spectrum revealing individual surface groups (shown in inset, top left) which provides a comparison of states.

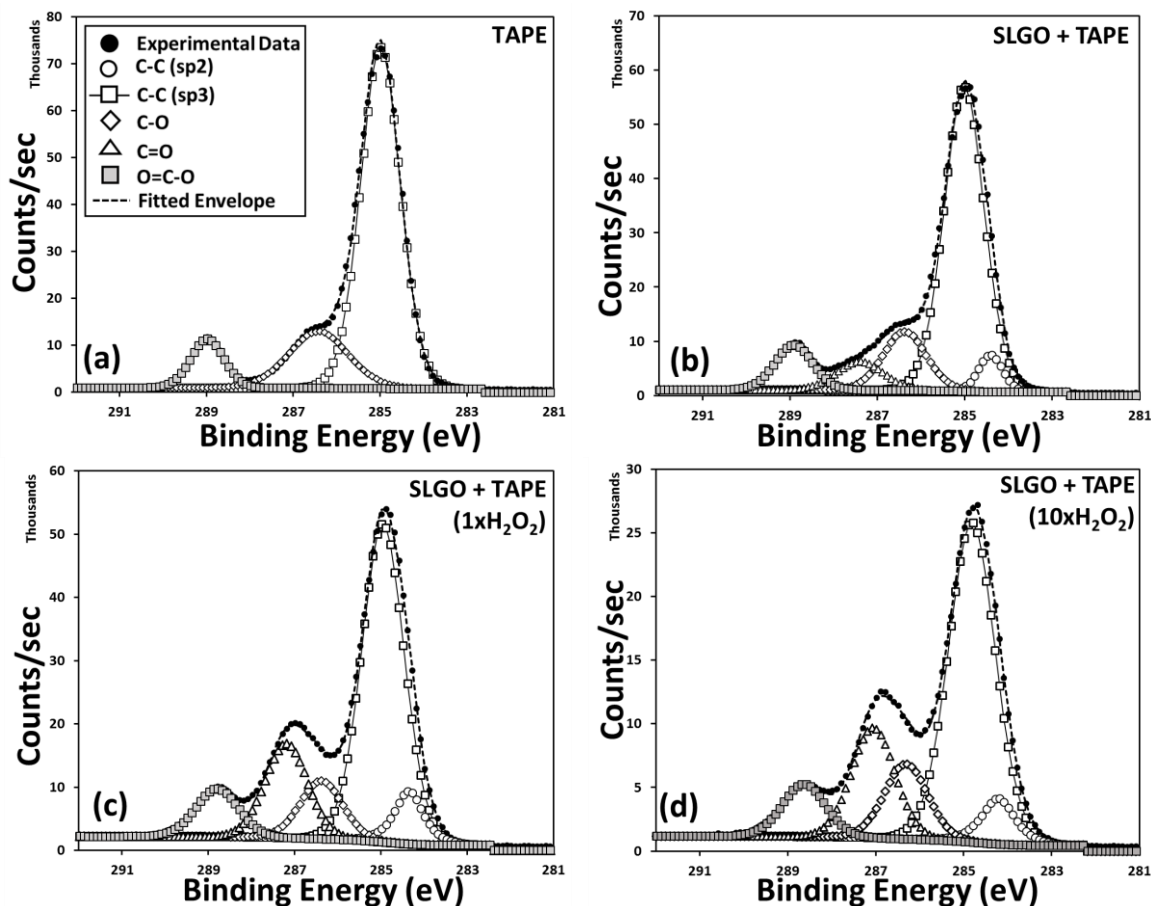


**Figure 6.** Kinetic study on the degradation of metaldehyde with SLGO and H<sub>2</sub>O<sub>2</sub>. Variation of the inverse of the concentration of metaldehyde with time follows a second order reaction

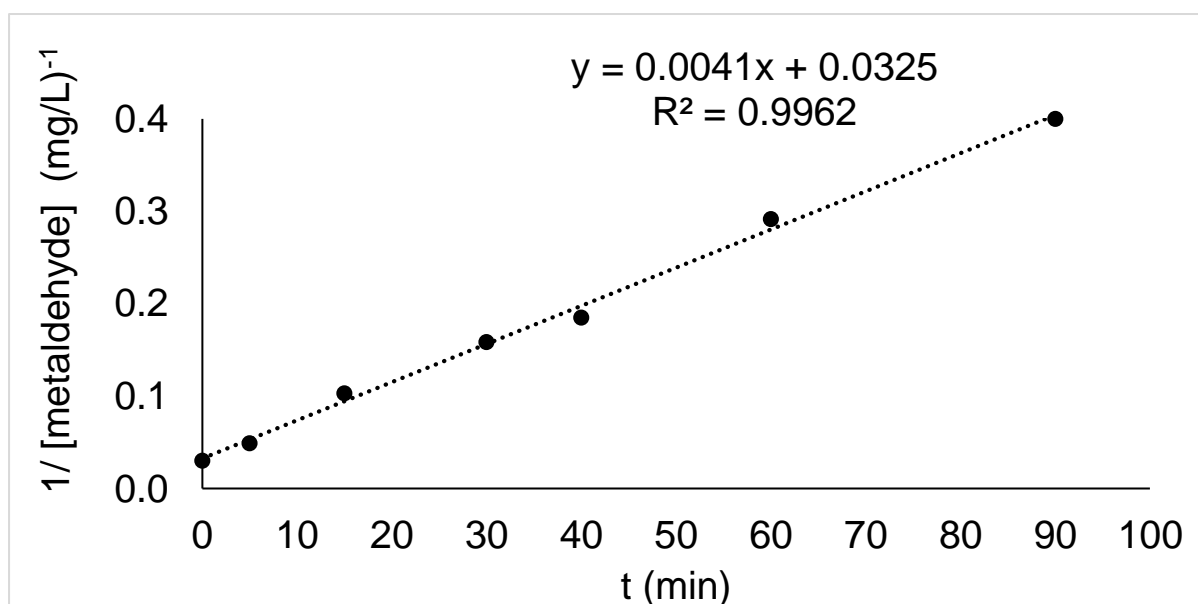
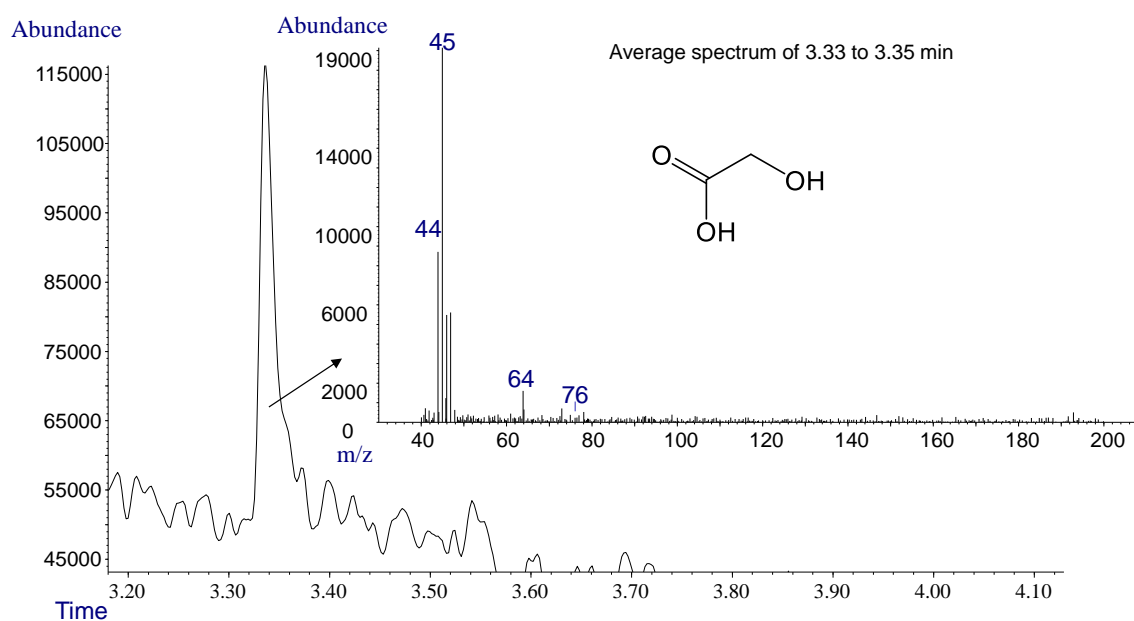


**Figure 7.** Analysis of metaldehyde degradation products. GC-MS chromatogram and spectra of the degradation products detected during the degradation of metaldehyde with SLGO after 15 and 30min of dosing the reaction mixture with 1% H<sub>2</sub>O<sub>2</sub>. The structure of the proposed degradation product is shown.



## Supplementary data

### Graphene Oxide-based Degradation of Metaldehyde: Effective Oxidation Through a Modified Fenton's Process

*Linh Viet Nguyen<sup>a,b,c</sup>, Rosa Busquets<sup>b,d\*</sup>, Santanu Ray<sup>b</sup> and Andrew B. Cundy<sup>b,e</sup>*

L.V. Nguyen

<sup>a</sup>Department of Physical and Environmental Sciences, University of Toronto, 1265 Military Trail, Toronto, ON, M1C 1A4, Canada.

<sup>b</sup>School of Environment and Technology, University of Brighton, Brighton, East Sussex, BN2 4GJ, United Kingdom.

<sup>c</sup>Ho Chi Minh University of Natural Resources and Environment, 236B Le Van Sy, Ward 1, Tan Binh District, Ho Chi Minh City, 70000, Vietnam. Present address.

E-mail: [Vietlinh.nguyen@mail.utoronto.ca](mailto:Vietlinh.nguyen@mail.utoronto.ca)

Dr. R. Busquets\*

<sup>d</sup>Faculty of Science, Engineering and Computing, Kingston University, Kingston Upon Thames, Surrey, KT1 2EE, United Kingdom. Present address.

Email: [R.Busquets@Kingston.ac.uk](mailto:R.Busquets@Kingston.ac.uk)

<sup>b</sup>School of Environment and Technology, University of Brighton, Brighton, East Sussex, BN2 4GJ, United Kingdom.

Dr. Santanu Ray

<sup>b</sup>School of Environment and Technology, University of Brighton, Brighton, East Sussex, BN2 4GJ, United Kingdom.

Email: [S.Ray4@Brighton.ac.uk](mailto:S.Ray4@Brighton.ac.uk)

Prof. Andrew B. Cundy

<sup>e</sup>School of Ocean and Earth Science, University of Southampton, Southampton, SO14 3ZH, United Kingdom. Present address.

Email: [A.Cundy@soton.ac.uk](mailto:A.Cundy@soton.ac.uk)

<sup>b</sup>School of Environment and Technology, University of Brighton, Brighton, East Sussex, BN2 4GJ, United Kingdom.

## **Supplementary data**

Supplementary data that consist of Materials and Methods (S1), Results and discussion (S2, S3) and Supplemental figures (Figures S1-S6).

### **S1 Materials and Methods**

Buffer solutions were used to study the individual effect of SLGO on metaldehyde (section 3.1) under controlled pH. First, the pH of SLGO suspended in aqueous solution was brought to the pKa of the selected weak conjugate acid-base pair with 0.1M NaOH. The suspension of SLGO in aqueous solution was favoured by sonication (5 minutes). Buffer solution, 10mM, was used to dissolve metaldehyde and was added (1:1) to the SLGO suspended in water followed by shaking (90 rpm, 25 °C for 48h) in an orbital shaker (model SI500 from Stuart Scientific, UK). Buffer solutions were pH 3 (10mM formic acid / ammonium formate), pH 5 (10 mM acetic acid/ ammonium acetate), pH 7 (1 mM and 10 mM sodium dihydrogenphosphate / disodium hydrogenphosphate), pH 9 (10 mM ammonia/ ammonium acetate) and pH 12 (10 mM sodium hydroxide). SLGO was at a final concentration of 375 mg/L. Further studies (section 3.2) used a final concentration of buffer of 100mM, in which metaldehyde was dissolved. Buffers with pH 8.5 were prepared with ammonia/ammonium acetate. Ultrapure water was obtained with an ELGA Purelab purification system (Veolia, UK). All other chemicals and solvents were of HPLC or analytical purity and were purchased from Fisher Scientific (UK).



## Results and Discussion

### S2. Interaction model for metaldehyde and SLGO in aqueous solution.

In order to investigate the molecular interaction between metaldehyde and SLGO, a chemical model of SLGO was constructed consisting of 6 hydroxyl groups and a carboxylic acid located at the edges of a planar sheet made of 16 benzenes, which is a hypothetical composition of SLGO. This was studied in aqueous solution at 298 K using MMF94 force field minimization and molecular dynamics. The results, illustrated in Figure S4, show that at minimum system energy configuration metaldehyde remains at a small distance from the nanocarbon but neither becomes adsorbed nor migrates away, which is in agreement with our previous results. The distance at which metaldehyde remains from the SLGO appears to be small enough to be affected by the  $\bullet\text{OH}$  generated on the SLGO by  $\text{H}_2\text{O}_2$  in the modified Fenton's process. We hypothesise that this distance between the contaminant and the SLGO may be critical in terms of achieving degradation. The degradation rate with the modified Fenton's process with SLGO would not be as effective for contaminants that remain over a critical distance from SLGO, or at too low concentrations of SLGO, both of which would limit the exposure of the contaminant to  $\bullet\text{OH}$ . This latter situation of limited mass transfer may explain the increasing degradation of the molluscicide observed when increasing the concentration of SLGO (Figure S5).

### **S3. Determination of the concentration of SLGO needed for the catalytic degradation of metaldehyde.**

Effective degradation of metaldehyde in the absence of  $\text{Fe}^{2+}$  was found at pH 5 and 8.5 using SLGO and  $\text{H}_2\text{O}_2$  (1%) (section 3.2). These conditions are advantageous mainly because the addition and subsequent separation of a homogenous catalyst (e.g. iron salts) would not be necessary. However, the application of the nanocatalyst at a larger scale has significant potential cost implications. In order to investigate the dependency of the degradation rate of metaldehyde on the amount of catalyst (i.e. SLGO) used, the efficiency of the degradation was studied at a range of SLGO concentrations suspended in solution in batch mode (Figure S5). The results showed that in the studied system (volume 10 ml) there was limited gain in metaldehyde degradation (present at 50 mg/L) at concentrations above 14.7 mg SLGO/L (ratio 3.4:1 between mass of metaldehyde and mass of SLGO). Thus, it could be estimated that at environmentally representative concentrations of 0.05  $\mu\text{g}$  metaldehyde /L (0.28 nM), 0.015  $\mu\text{g}$  SLGO/L (85 pM) would be required for metaldehyde degradation (this amount was not confirmed experimentally because a volume of water far too large for batch experimentation would be required for an amount of SLGO that could be weighed accurately with an analytical balance). However, since contact between the catalyst and the molluscicide is necessary, a batch system with effective stirring or flow through mode with turbulent flow that favours contact between SLGO and metaldehyde would improve the performance. This is however not an issue specific to SLGO but applies for all heterogeneous catalysts used to treat large volumes of water. Hence, stirring/ agitation, contact time and SLGO dosage would need to be optimized for water treatment in an upscaled system in water treatment facilities so that mass transfer does not become a limiting step.

## Supplemental figures

**Figure S1.** Figure 1 S. SEM micrographs obtained from the starting SLGO at two different magnifications (a, b); SLGO treated with 1%  $\text{H}_2\text{O}_2$  (1 cycle) (c); and SLGO treated with 1%  $\text{H}_2\text{O}_2$  (10 cycles) (d).

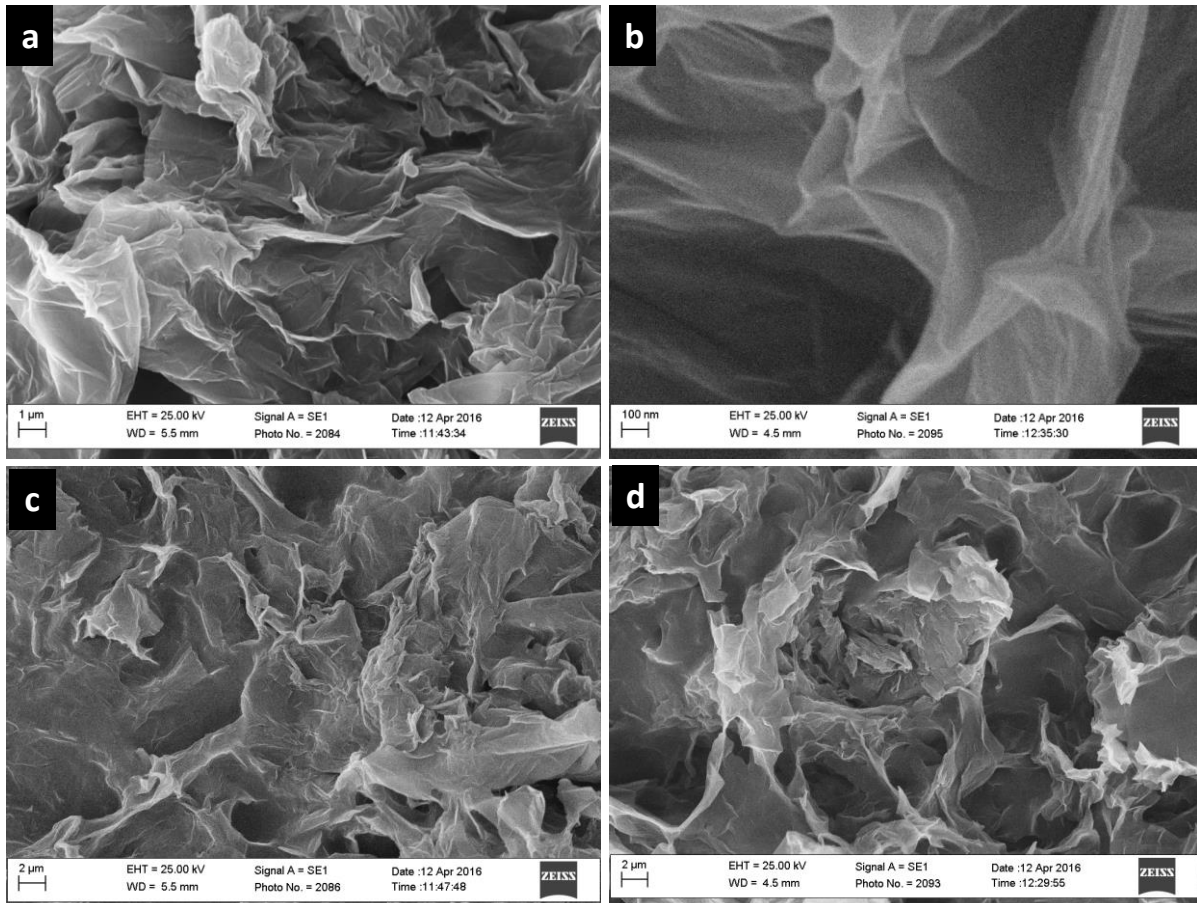


**Figure S2.** Images of the immobilised SLGO on cellulose tape. a) and c) show SLGO immobilised on cellulose tape in a flask before the introduction of water contaminated with metaldehyde; b) SLGO immobilised on cellulose tape before folding into the flask.

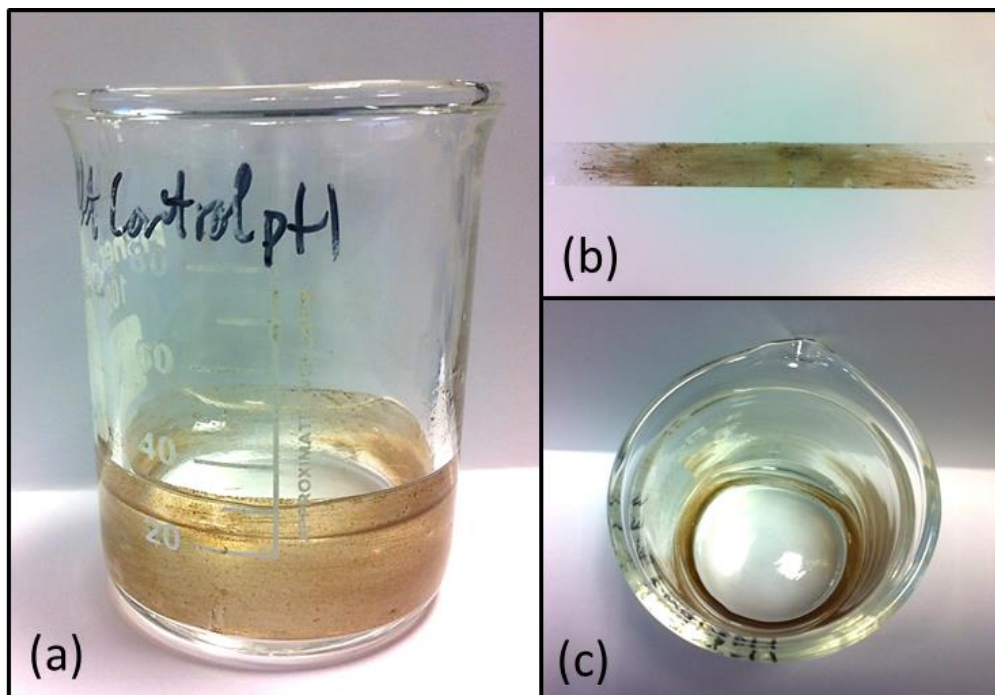


**Figure S3.** Effect of pH, and pH and SLGO on the concentration of metaldehyde in solution (starting concentration 41 mg metaldehyde/L and 375 mg SLGO/L). Experimental conditions are detailed in section 2. Error bars correspond to the standard deviation for n=3.

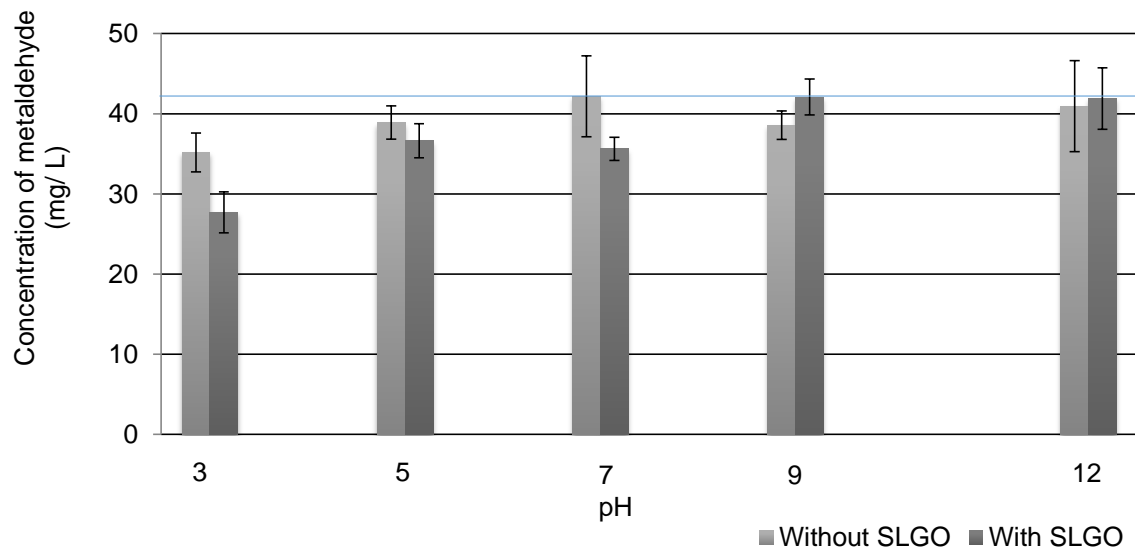


**Figure S4.** Molecular dynamics model (MMFF94) showing a minimum energy configuration between a simulated graphene sheet and metaldehyde in aqueous solution.

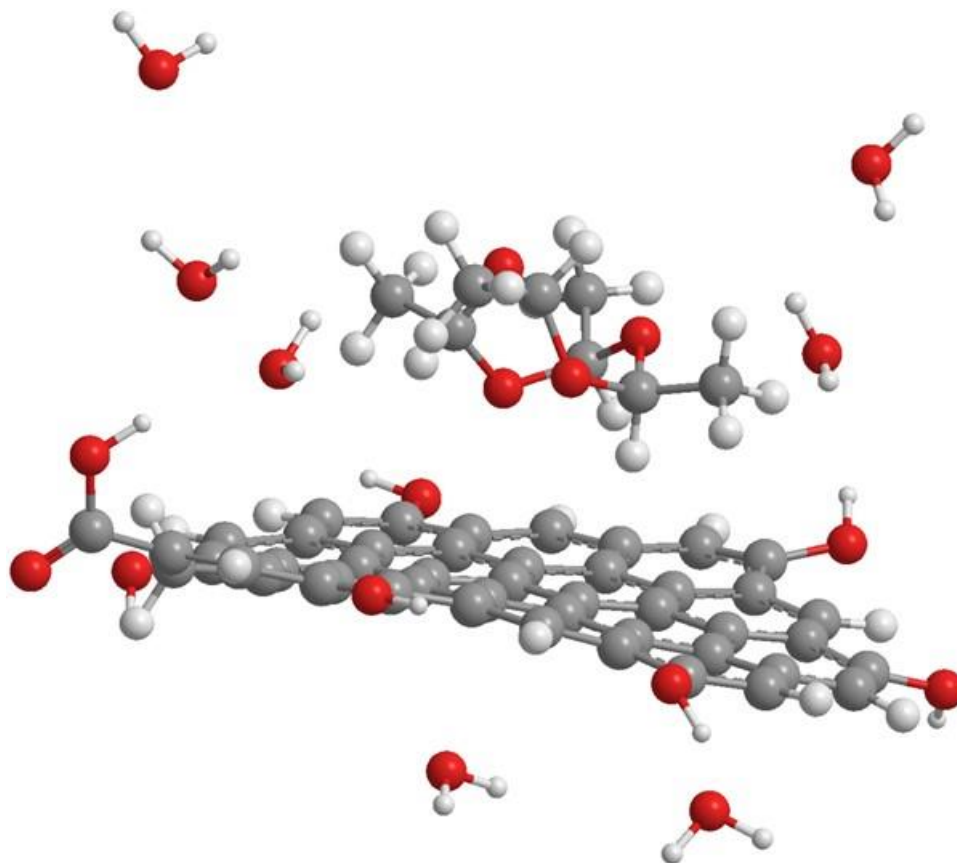


**Figure S5.** Effect of hydrogen peroxide concentration on the degradation of metaldehyde (n=3). The experiments used 50 mg metaldehyde /L adjusted to pH 8.5 (shaken on an orbital shaker at 90 rpm, at 25 °C for 35 minutes), with 0% (control), 1%, 5% and 10% H<sub>2</sub>O<sub>2</sub>. No SLGO was added. The structure of metaldehyde following MMFF94 minimisation treatment is provided.

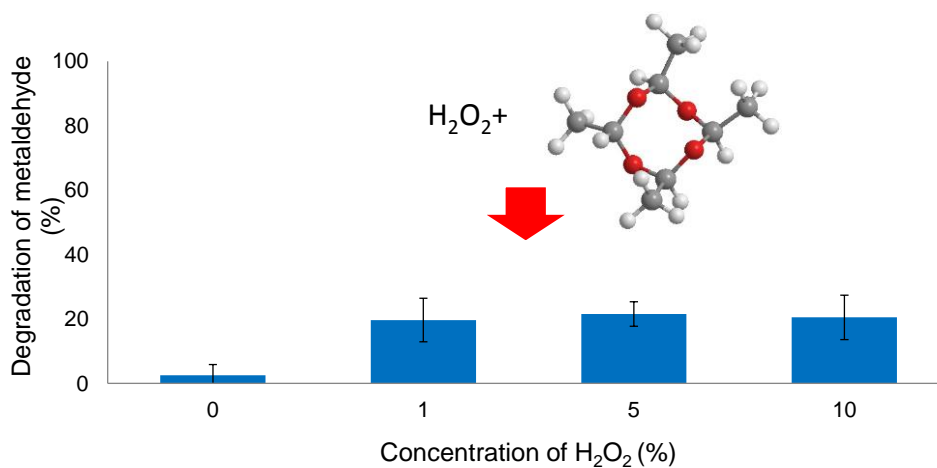


**Figure S6.** Dependence of the degradation of metaldehyde on concentration of SLGO in batch mode. SLGO was suspended in 100 mM ammonium acetate/acetic acid buffer at pH 5 containing 50 mg metaldehyde/L and sonicated (5 minutes). H<sub>2</sub>O<sub>2</sub> (1%) was added to the mixture, which had a total volume of 10 ml and was shaken in an orbital shaker at 90 rpm, 25°C for 60 minutes. The system with suspended SLGO in one of the study conditions is displayed.

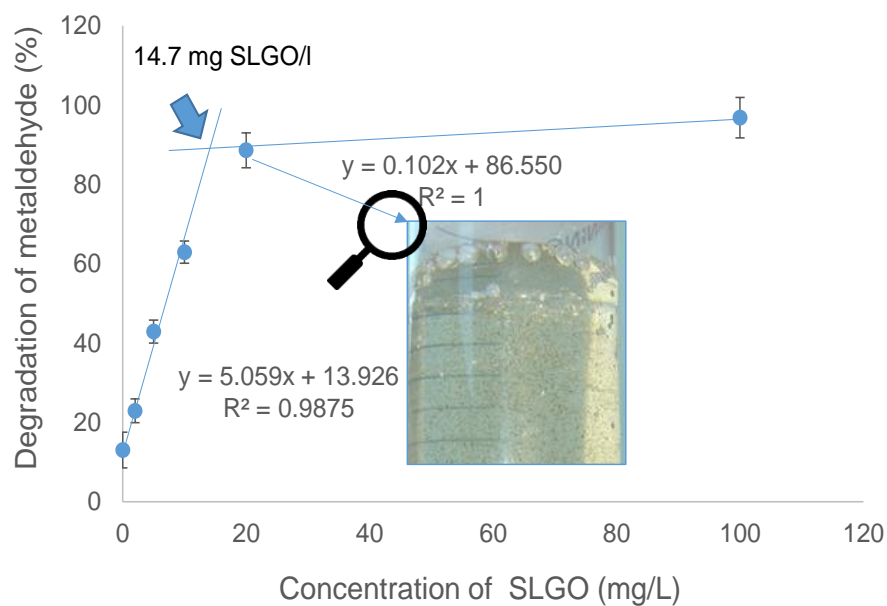




**Figure S7** FTIR spectra from the cellulose tape (a), SLGO immobilised onto tape (b); SLGO treated with 1% H<sub>2</sub>O<sub>2</sub> (1 cycle) (c); and SLGO treated with 1% H<sub>2</sub>O<sub>2</sub> (10 cycles) (d). The carbonyl, C-O and C=C stretch have been indicated.

